Applied Physics Letters

RESEARCH ARTICLE | APRIL 14 2023

Molecular *p*-doping induced dielectric constant increase of polythiophene films determined by impedance spectroscopy

Ross Warren ; Paul W. M. Blom ; Norbert Koch

Appl. Phys. Lett. 122, 152108 (2023)
https://doi.org/10.1063/5.0146194

Applied Physics Letters ARTICLE scitation.org/journal/apl

Molecular *p*-doping induced dielectric constant increase of polythiophene films determined by impedance spectroscopy

Cite as: Appl. Phys. Lett. **122**, 152108 (2023); doi: 10.1063/5.0146194
Submitted: 11 February 2023 · Accepted: 1 April 2023 ·
Published Online: 14 April 2023

View Online Export Citation CrossMark

Ross Warren,[1] Paul W. M. Blom,[2] and Norbert Koch[1,3,a)]

AFFILIATIONS

[1]Institut für Physik & IRIS Adlershof, Humboldt-Universität zu Berlin, Berlin 12489, Germany
[2]Max Planck Institute for Polymer Research, Mainz 55128, Germany
[3]Helmholtz-Zentrum Berlin für Materialien und Energie GmbH, Berlin 12489, Germany

[a)]Author to whom correspondence should be addressed: nkoch@physik.hu-berlin.de

ABSTRACT

The dielectric constant (ε_r) is a fundamental material parameter that governs charge transfer processes in organic semiconductors, yet its value is often assumed rather than measured. Here, we use impedance spectroscopy to determine ε_r in regioregular poly(3-hexylthiophen-2,5-diyl) (P3HT) thin films *p*-doped with the molecular dopants hexafluoro-tetracyanonaphthoquinodimethane and 2,3,5,6-tetrafluoro-7,7,8,8-tetracyanoquinodimethane (F4TCNQ). We fit the impedance spectra using a single RC circuit model to determine the frequency-dependent capacitance and extract ε_r. The value of the dielectric constant increases by around two-thirds from 2.9 ± 0.1 (undoped polymer) to 4.9 ± 0.6 on the addition of one F4TCNQ molecule per 500 P3HT monomer units. In contrast, the addition of the weak dopant 7,7,8,8-tetracyanoquinodimethane (TCNQ), which does not undergo ground state charge transfer with P3HT, has no effect on the dielectric constant. Our results support the hypothesis that molecular doping has a considerable impact on the materials dielectric constant via polarizable host-dopant complexes.

The dielectric constant ε_r (or the static relative permittivity) describes the ability of a material to screen a charge, dampening the strength of its electric field. It is defined as the permittivity of a material divided by the permittivity of free space. The lower the dielectric constant, the less the material will screen an electric field. Consequently, in lower dielectric materials, the Coulomb attraction between holes and electrons is stronger. Organic semiconductors are an example of such materials, with dielectric constants reported in the range of 2–5.[1–3] The low dielectric constant of organic semiconductors promotes their pronounced excitonic character and plays an important role when it comes to applications in devices. For example, in solar cells, low dielectric constant values are associated with recombination-based energy losses,[4–6] as the photo-excited electron–hole pairs must separate from one another or else recombine to the ground state. In organic field-effect transistors, Coulomb interactions between charge carriers can impact the mobility[7] and, therefore, switching speed of the device.[8] Furthermore, many techniques used to characterize organic electronic materials require the dielectric constant to be known, e.g., in Mott–Schottky analysis[9] and mobility measurements using the space-charge limited current method.[10] Despite the importance of the dielectric constant for both the characterization and application of organic semiconductors, an approximate value of $\varepsilon_r = 3$ is often assumed rather than measured.

For the molecular doping of organic semiconductors, that is the controlled introduction of impurities to increase carrier density, and thus the conductivity, the dielectric constant plays a particularly critical role. To understand why, the process by which a molecular dopant generates mobile carriers can be broken down into two steps: (i) initial charge transfer between the host and dopant, followed by (ii) charge dissociation. For this latter step, the separation barrier is determined by the Coulomb interaction between the ionized dopant and the charge on the host semiconductor. Calculations[11,12] and photoemission measurements[13] suggest that this binding energy is in the region of 0.45–0.65 eV, which is much larger than the thermal energy at room temperature. This raises the question, how are free charge carriers generated in doped organic semiconductors? The most cited explanations include a Coulomb potential overlap between nearby

dopant ions,[14] energetic disorder,[15,16] and long-range electrostatic interactions.[11,17]

Recently, Comin *et al.*[18] put forward an alternative proposal that the release of charge carriers can be accounted for by changes in dielectric constant as a function of doping concentration. With first principles and microelectrostatic calculations, they demonstrated that the highly polarizable host-dopant complexes contribute to a screening phenomenon, which lowers the energy barrier for charge separation to within the thermal energy at room temperature. Although this mechanism of carrier release is consistent with experimental measurements of temperature-activated conductivity, the change in dielectric constant as a function of dopant concentration in organic semiconductors has yet to be directly determined.

In this study, we use impedance spectroscopy to assess the dielectric constant as a function of dopant concentration in thin films of the organic semiconductor regioregular poly(3-hexylthiophen-2,5-diyl) (P3HT) *p*-doped with molecular electron acceptors hexafluorotetracyanonaphthoquinodimethane (F6TCNNQ) and 2,3,5,6-tetrafluoro-7,7,8,8-tetracyanoquinodimethane (F4TCNQ). We present Nyquist plots over a range of DC bias voltages, up to a dopant concentration of 500 P3HT monomer units per dopant molecule. The impedance data are modeled using a single RC circuit, allowing the frequency-dependent capacitance and dielectric constant to be determined. We find that the dielectric constant increases as a function of dopant concentration, from 2.9 for the undoped P3HT to between 4 and 5 for the highest doping levels investigated here. Our control experiment shows no increase in dielectric constant for P3HT doped with the weaker electron acceptor 7,7,8,8-tetracyanoquinodimethane (TCNQ), where ground state charge transfer, and thus doping, does not occur.[19] This demonstration of the doping induced increase in ε_r confirms recent theoretical work[18] and underpins the need for better understanding of fundamental processes that occur in organic semiconductors upon doping.

The experimental methods proceed as follows. P3HT is dissolved in chlorobenzene at a concentration of 20 mg/ml. F6TCNNQ and TCNQ are dissolved in chlorobenzene at a concentration of 2 mg/ml. F4TCNQ is dissolved in chloroform at a concentration of 1 mg/ml. Indium-tin-oxide (ITO) coated glass substrates are cleaned by sonication in water, acetone, and then isopropanol, followed by treatment with an O_2 plasma cleaner. A poly(3,4-ethylenedioxythiophene):polystyrene sulfonate (PEDOT:PSS) layer is spin-coated at 3000 rpm for 60 s and dried at 150 °C for 15 min. The polymer layers are spin-coated in a nitrogen-filled glovebox at 600–800 rpm for 60 s, followed by 3000 rpm for 20 s. The 1.77 mm^2 Al electrode (~100 nm thick) and Sm (8 nm thick) interlayer are thermally evaporated at a base pressure of $< 10^{-6}$ mbar. The resulting Schottky diodes are characterized within the glovebox (to minimize water and oxygen exposure) using an impedance spectrometer (Solartron Analytical ModuLab XM MAT 1 MHz). Film thicknesses are determined by measuring across a scratch in the film using an atomic force microscope (Bruker AFM Multimode 8). The doped layer thicknesses are in the range of 100–120 nm with standard deviations in the range of 1–2 nm over seven measurements.

Figure 1 shows the current–voltage characteristics of (a) P3HT:F6TCNNQ, (b) P3HT:F4TCNQ, and (c) P3HT:TCNQ Schottky diodes with ratios of 5000:1, 1000:1, and 500:1 P3HT monomer units to dopant molecules. The PEDOT:PSS layer is used to reduce the surface roughness as compared to the bare ITO, therefore helping to achieve an even thickness of the active layer.[20] Additionally, for the P3HT:F4TCNQ devices, an 8 nm layer of Sm is used to protect the organic layer against metal diffusion during the Al deposition,[21] improving device reproducibility. In reverse bias, the current is limited by the injection barrier between the P3HT, with an ionization energy of around 4.6 eV,[22] and the aluminum contact, with a work function of around 4.3 eV.[23] For the devices doped with F6TCNNQ, the reverse bias current increases. This happens because there is a reduction in the injection barrier height as the free carrier density increases due to the addition of the dopant.[24] In contrast, the introduction of TCNQ has no effect on the current in reverse bias with the current remaining comparable to the undoped case. This is as expected because free carriers should not be generated by the addition of TCNQ. Charge transfer is energetically unfavorable as the electron affinity of TCNQ, at around 4.23 eV,[22] is lower than the ionization energy of the P3HT.

To determine the effect of doping on the dielectric constant of the polymer semiconductor, we perform impedance measurements. We take into account guidelines specific for organic semiconducting

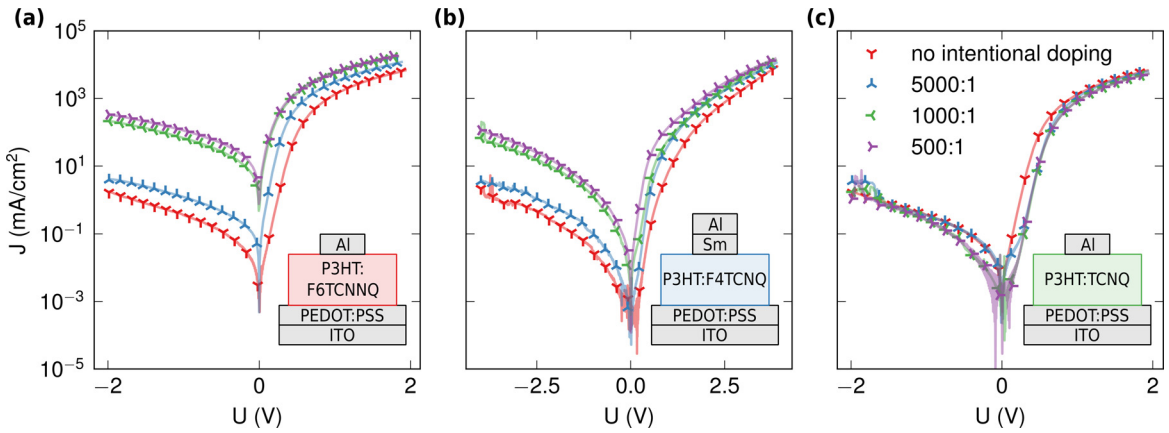

FIG. 1. Current–voltage characteristics of rr-P3HT diodes p-doped at different dopant concentrations, with (a) F6TCNNQ, (b) F4TCNQ, and (c) TCNQ. The dopant concentrations are given as a ratio of dopant molecules to P3HT monomer units. The diagrams inset show the device stack.

materials given by von Hauf[25] and Hughes *et al.*[1] Figure 2 shows the Nyquist plots, that is the real part against the imaginary part of the measured impedance, for the pristine P3HT device and the devices doped with F6TCNNQ. Each device is measured with a DC bias of −0.5, −1.0, and −1.5 V, to prevent charge carriers diffusing from the contacts and ensure a depleted active layer (discussed in further detail later).

The plots show concentric semi-circles, which decrease in radius as the DC bias decreases. Only one clear semi-circular feature is present in each sweep, indicating that an equivalent circuit model based on a single RC circuit element will be sufficient to reproduce the experimental data. We choose to also include a resistor and an inductor in series, representing the AC resistance and inductance for the test setup. The model fitting is performed by non-linear least squares regression,[26] via the *impedance.py* python package.[27] The best fits for each of the devices are shown in Fig. 2 as the dashed lines.

We note that this analysis using an equivalent circuit model based on a single RC element assumes that the depletion region extends across the entire active layer of the device. If the depletion region did not extend across the device, then we would expect to see a second semi-circular feature in the Nyquist plot, as Chen *et al.*[28] observed for their *p*-doped Schottky diodes. To ensure our model's validity, we have two levers to pull—the dopant concentration and the DC bias. Estimating the depletion width, using Poisson's equation, guides us to keep the dopant concentration below 300:1 and consider DC biases of at least –0.5 V. Experimentally, we find that the capacitance against DC bias, shown in the supplementary material in Fig. SI 2, saturates at around –0.5 V, suggesting that at this point, the device is depleted.

To extract the dielectric constant, we first determine the frequency-dependent capacitance, given by

$$C = \frac{-1}{\omega}\left[\frac{Z'' - \omega L}{(Z' - R_s)^2 + (Z'' - \omega L)^2}\right],$$

where Z' is the real part of the impedance, Z'' is the imaginary part of the impedance, ω is the angular frequency ($\omega = 2\pi f$), f is the linear frequency, L is the setup inductance, and R_s is the AC series resistance.[1] From the capacitance, the dielectric constant is given by

$$\varepsilon_r = \frac{C \cdot d}{\varepsilon_0 \cdot A},$$

where d is the polymer layer thickness and A is the device area.

Figure 3(a) shows the capacitance spectra for P3HT:F6TCNNQ as a function of frequency for each dopant concentration (see Fig. S2 in the supplementary material for the capacitance spectra of TCNQ and F4TCNQ doped diodes). For the neat P3HT devices, that is with no intentional doping, the capacitance gives a frequency-independent dielectric constant of 2.9 ± 0.1, which is in good agreement with other published work.[1] With increasing dopant concentration, the capacitance increases over all parts of the frequency spectrum. The increase in capacitance is larger at lower frequencies (below 10^4 Hz) than at higher frequencies, which makes determining a geometric capacitance more difficult as compared to the frequency-independent capacitance of the non-doped case. A reason for an increase in capacitance at lower frequencies includes leakage of charges from the electrodes into the active layer.[1] Therefore, to determine a dielectric constant, we take the mean of the capacitance in the higher range of the spectrum, between 10^5 and 10^6 Hz, where charge leakage has less impact.

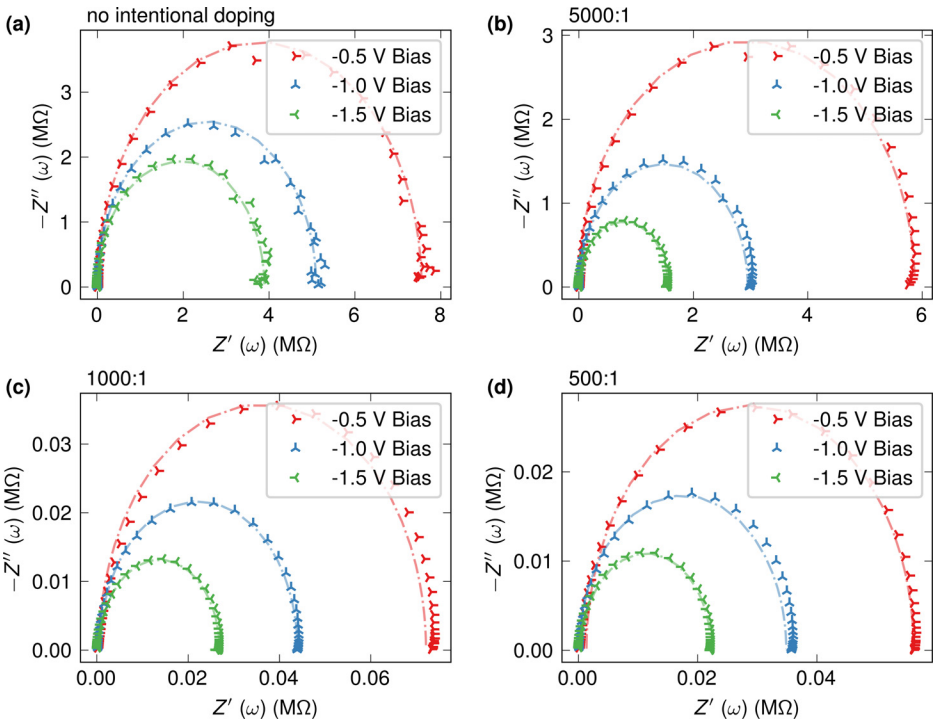

FIG. 2. Nyquist plots of the impedance spectra. The dashed lines show the equivalent circuit model fit using a single RC element. The points are the experimental data. (a) The neat P3HT with no intentional doping, and (b)–(d) P3HT:F6TCNNQ at a doping ratio of 5000:1, 1000:1, and 500:1 P3HT monomer units to dopant molecules, respectively.

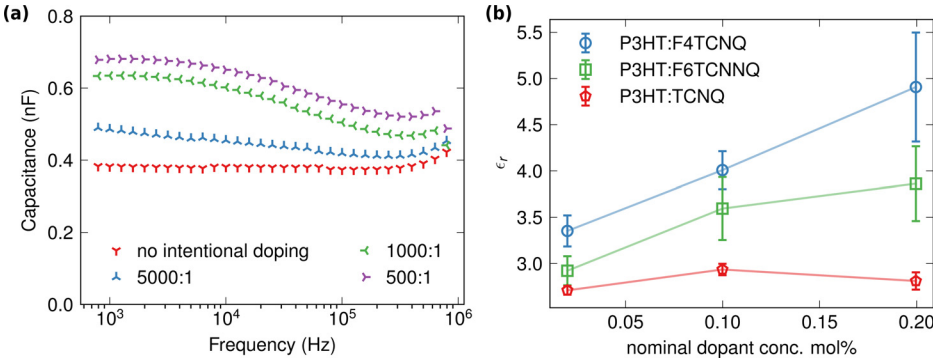

FIG. 3. Capacitance spectra and dielectric constant with varying doping concentration. (a) Capacitance as a function of frequency at a DC bias of −0.5 V for diodes of P3HT:F6TCNNQ. (b) Dielectric constant, at a DC bias of −0.5 V, against nominal dopant concentration for P3HT diodes p-doped with TCNQ, F4TCNQ, and F6TCNNQ. The values of dielectric constant are determined by taking the mean capacitance between 10^5 and 10^6 Hz, with the error bar representing the standard deviation in combination with the uncertainty in film thicknesses.

We plot the dielectric constant against the doping concentration in Fig. 3(b), with the values calculated using the mean capacitance. The error bars reflect the standard deviation of the capacitance in combination with the standard deviation in film thicknesses. The dielectric constant increases from 2.9 ± 0.1 in undoped P3HT to 3.9 ± 0.4 for the device p-doped at 500:1 F6TCNNQ, and 4.9 ± 0.6 for F4TCNQ. With TCNQ as the p-dopant in the P3HT layer, there is no clear increase in the dielectric constant.

Finally, we convert nominal dopant concentration, that is the concentration as calculated by taking the volume ratios between the polymer and dopant solutions, to carrier concentration N_d, using Mott–Schottky analysis (see supplementary material Figs. 3 and 4 for the plots of C^{-2} against DC bias). Along with N_d, we also find built-in potentials of around 0.7 V for our PEDOT:PSS/semiconductor/Al devices, and around 2.5–3.1 V for our PEDOT:PSS/semiconductor/Sm/Al devices. These values are in good agreement with the expected built-in potentials considering the contact work function values.[23,29,30] We plot the carrier concentration N_d against extracted dielectric constant in Fig. 4. Both sets of data from the P3HT:F4TCNQ and P3HT:F6TCNNQ devices show a linear relationship between the dielectric constant and carrier density. Taking a simple model of Castellan and Seitz[31] of spherical hydrogen-like dopant impurities isotropically distributed in a host semiconductor, the change in dielectric constant is linear over the dopant range presented here. The model fits are shown in Fig. 4 as dashed lines, with the fitting parameter of the dopant's polarizability reported in the legend. All in all, we conclude that the addition of molecular dopants to our polymer semiconductor leads to an increase in the dielectric constant. This is in line with observations on inorganic semiconductors,[32] and as predicted by recent theoretical work from Comin *et al.*[18]

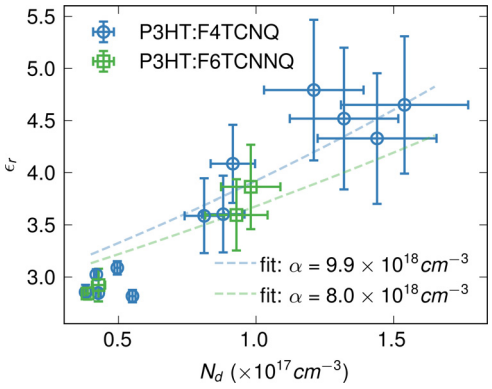

FIG. 4. Plot of the dielectric constant ε_r against carrier concentration N_d for the P3HT diodes p-doped with F4TCNQ and F6TCNNQ. The model fits are shown as dashed lines.

We anticipate that the dielectric constant continues to increase as the dopant concentration increases. In fact, the calculations from Comin *et al.*[18] suggested a tenfold increase in dielectric constant at a dopant concentration of 8%. Although our measurements only go up to a dopant concentration of 500:1 (~0.2%), the roughly two-thirds enhancement of the dielectric constant lends support to the hypothesis that doping has a considerable impact on the material's relative permittivity. Our impedance analysis based on a single RC circuit element places an upper limit on the dopant concentration we can study; however, the concentration range presented remains relevant for Schottky diodes. To directly determine the dielectric constant beyond this range requires the use of microwaves and transmission lines. We hope our study leads to further investigations of the dielectric constant in other doped organic semiconductors, and to the pursuit of the measurement over an increased dopant concentration range.

See the supplementary material for the capacitance measurements and Mott–Schottky analysis.

This work in Berlin was supported by the Deutsche Forschungsgemeinschaft (Project No. 182087777-SFB951).

AUTHOR DECLARATIONS

Conflict of Interest

The authors have no conflicts to disclose.

Author Contributions

Ross Warren: Conceptualization (supporting); Data curation (lead); Formal analysis (lead); Investigation (lead); Methodology (equal); Writing – original draft (lead); Writing – review & editing (supporting). **Paul W. M. Blom:** Formal analysis (supporting); Methodology (supporting); Writing – review & editing (equal). **Norbert Koch:** Conceptualization (equal); Funding acquisition (lead); Resources (lead); Supervision (equal); Writing – review & editing (equal).

DATA AVAILABILITY

The data that support the findings of this study are available from the corresponding author upon reasonable request.

REFERENCES

[1]M. P. Hughes, K. D. Rosenthal, N. A. Ran, M. Seifrid, G. C. Bazan, and T. Q. Nguyen, Adv. Funct. Mater. **28**, 1801542 (2018).
[2]C. H. Kim, O. Yaghmazadeh, D. Tondelier, Y. B. Jeong, Y. Bonnassieux, and G. Horowitz, J. Appl. Phys. **109**, 083710 (2011).
[3]K. Ortstein, S. Hutsch, M. Hambsch, K. Tvingstedt, B. Wegner, J. Benduhn, J. Kublitski, M. Schwarze, S. Schellhammer, F. Talnack, A. Vogt, P. Bauerle, N. Koch, S. C. B. Mannsfeld, H. Kleeman, F. Ortmann, and K. Leo, Nat. Mater. **20**(10), 1407–1413 (2021).
[4]L. J. A. Koster, S. E. Shaheen, and J. C. Hummelen, Adv. Energy Mater. **2**, 1246–1253 (2012).
[5]S. Chen, S.-W. Tsang, T.-H. Lai, J. R. Reynolds, and F. So, Adv. Mater. **26**, 6125–6131 (2014).
[6]S. Rousseva, H. den Besten, F. S. van Kooij, E. L. Doting, N. Y. Doumon, E. Douvogianni, L. J. Anton Koster, and J. C. Hummelen, J. Phys. Chem. C **124**, 8633–8638 (2020).
[7]F. Liu, H. van Eersel, B. Xu, J. G. Wilbers, M. P. de Jong, W. G. van der Wiel, P. A. Bobbert, and R. Coehoorn, Phys. Rev. B **96**, 205203 (2017).
[8]G. Gelinck, P. Heremans, K. Nomoto, and T. D. Anthopoulos, Adv. Mater. **22**, 3778–3798 (2010).
[9]T. Kirchartz, W. Gong, S. A. Hawks, T. Agostinelli, R. C. I. MacKenzie, Y. Yang, and J. Nelson, J. Phys. Chem. C **116**, 7672–7680 (2012).
[10]J. C. Blakesley, F. A. Castro, W. Kylberg, G. F. A. Dibb, C. Arantes, R. Valaski, M. Cremona, J. S. Kim, and J.-S. Kim, Org. Electron. **15**, 1263–1272 (2014).
[11]A. Privitera, G. Londi, M. Riede, G. D'Avino, and D. Beljonne, Adv. Funct. Mater. **30**, 2004600 (2020).
[12]J. Li, I. Duchemin, O. M. Roscioni, P. Friederich, M. Anderson, E. Da Como, G. Kociok-Kohn, W. Wenzel, C. Zannoni, D. Beljonne, X. Blase, and G. D'Avino, Mater. Horiz. **6**, 107–114 (2019).
[13]C. Gaul, S. Hutsch, M. Schwarze, K. S. Schellhammer, F. Bussolotti, S. Kera, G. Cuniberti, K. Leo, and F. Ortmann, Nat. Mater. **17**, 439–444 (2018).
[14]A. Mityashin, Y. Olivier, T. van Regemorter, C. Rolin, S. Verlaak, N. G. Martinelli, D. Beljonne, J. Cornil, J. Genoe, and P. Heremans, Adv. Mater. **24**, 1535–1539 (2012).
[15]M. L. Tietze, J. Benduhn, P. Pahner, B. Nell, M. Schwarze, H. Kleemann, M. Krammer, K. Zojer, K. Vandewal, and K. Leo, Nat. Commun. **9**, 1182 (2018).
[16]A. Fediai, A. Emering, F. Symalla, and W. Wenzel, Phys. Chem. Chem. Phys. **22**, 10256–10264 (2020).
[17]R. Warren, A. Privitera, P. Kaienburg, A. E. Lauritzen, O. Thimm, J. Nelson, and M. K. Riede, Nat. Commun. **10**, 5538 (2019).
[18]M. Comin, S. Fratini, X. Blase, and G. D'Avino, Adv. Mater. **34**, 2105376 (2022).
[19]H. Méndez, G. Heimel, S. Winkler, J. Frisch, A. Opitz, K. Sauer, B. Wegner, M. Oehzelt, C. Rothel, S. Duhm, D. Többens, N. Koch, and I. Salzmann, Nat. Commun. **6**, 8560 (2015).
[20]J. Brebels, J. V. Manca, L. Lutsen, D. Vanderzande, and W. Maes, J. Mater. Chem. A **5**, 24037–24050 (2017).
[21]J. Wagner, M. Gruber, A. Wilke, Y. Tanaka, K. Topczak, A. Steindamm, U. Hörmann, A. Opitz, Y. Nakayama, H. Ishii, J. Pflaum, N. Koch, and W. Brütting, J. Appl. Phys. **111**(5), 054509 (2012).
[22]J. Frisch, A. Vollmer, J. P. Rabe, and N. Koch, Org. Electron. **12**, 916–922 (2011).
[23]M. Stössel, J. Staudigel, F. Steuber, J. Simmerer, and A. Winnacker, Appl. Phys. Mater. Sci. Process. **68**, 387–390 (1999).
[24]Y. Zhang and P. W. M. Blom, Appl. Phys. Lett. **97**, 083303 (2010).
[25]E. von Hauff, J. Phys. Chem. C **123**, 11329–11346 (2019).
[26]P. Virtanen, R. Gommers, T. E. Oliphant *et al.*, Nat. Methods **17**, 261–272 (2020).
[27]M. D. Murbach, B. Gerwe, N. Dawson-Elli, and L. Tsui, J. Open Source Softw. **5**, 2349 (2020).
[28]C.-C. Chen, B.-C. Huang, M.-S. Lin, Y.-J. Lu, T.-Y. Cho, C.-H. Chang, K.-C. Tien, S.-H. Liu, T.-H. Ke, and C.-C. Wu, Org. Electron. **11**, 1901–1908 (2010).
[29]A. E. Mansour, H. Kim, S. Park, T. Schultz, D. X. Cao, T. O. Nguyen, W. Brütting, A. Opitz, and N. Koch, Adv. Elect. Mater. **6**, 2000408 (2020).
[30]N. Koch, J. Ghijsen, R. L. Johnson, J. Schwartz, J. J. Pireaux, and A. Kahn, J. Phys. Chem. B **106**(16), 4192–4196 (2002).
[31]G. W. Castellan and F. Seitz, *Semiconducting Materials* (Butterworths, London, 1951).
[32]S. Dhar and A. H. Marshak, Solid-State Electron. **28**(8), 763–766 (1985).